Executive Summary of the Thesis Entitled

Processing and Characterization of In-Situ Aluminium Matrix Composite by Stir Casting Method

is submitted to

THE MAHARAJA SAYAJIRAO UNIVERSITY OF BARODA

in the partial fulfillment of the requirements for the degree of

Doctor of Philosophy

in

METALLURGICAL AND MATERIALS ENGINEERING

by

Hemantkumar Narendrabhai Panchal

Research Guide

Dr. Vandana J. Rao

Metallurgical and Materials Engineering Department
Faculty of Technology and Engineering
The Maharaja Sayajirao University of Baroda
Vadodara – 390001, Gujarat (India)

2022-2023

Table of Contents

Certificate ii

Anti-Plagiarism Certificate iii

Declaration of Authorship iv

Acknowledgement v

Abstract vi

List of Figures **xii**

List of Tables **xviii**

1 INTRODUCTION **1**

1.1 Background 1

1.2 Problem Formulation 2

1.3 Objectives of the work 3

1.4 Scope of the work 4

1.5 Research findings 5

1.6 Research methodology 5

1.7 Thesis layout 6

2 LITERATURE REVIEW **8**

2.1 Composite Material 8

2.2 Classification of composite materials 9

2.2.1 Based on matrix 10

2.2.2 Based on reinforcement 13

2.2.3 The rule of mixture 16

2.2.4 Other types of composite materials 17

2.3 Manufacturing of the composite materials 18
2.3.1 Solid state process (Powder metallurgy route) 20
2.3.2 Liquid state process 27

2.4 Equilibrium diagrams of important system 38
2.4.1 Binary System: Al-Mg 38
2.4.2 Binary System: Al-Mn 39
2.4.3 Ternary System: Al-Mg-Mn 40

2.5 Solidification of Composite 42
2.5.1 Undercooling 45
2.5.2 Nucleation 46
2.5.3 Growth and solidification front 48

2.6 Aluminium Matrix Composites (AMCs) 51
2.6.1 About Aluminium 52
2.6.2 Reinforcement used to make AMCs 66
2.6.3 Ex-situ method: 67
2.6.4 In-situ method: 68

2.7 Application of composites 73
2.8 Literature review of technical papers 73

3 EXPERIMENTAL WORK **84**

3.1 Experimental set up and its description 86

3.1.1 Electrical resistance Al melting furnace: 86

3.2 Experimental Procedure 90

3.2.1 Phase I: Optimization of Magnesium content in CPA 90
3.2.2 Phase II: Effect of variation of MnO_2 content by changing its addition sequence into CPA 93
3.2.3 Phase III: Effect of variation of MnO_2 by changing its addition sequence along with optimised magnesium metal from phase I into CPA 97

3.3 Standard steps followed for metallography of composite samples 101
3.3.1 Sampling 101

3.3.2 Grinding 101
3.3.3 Polishing 102

3.4 Difficulty in melting of Aluminium and its remedies 102
3.4.1 Drossing 102
3.4.2 Gas absorption 103
3.4.3 Fluxing and flushing or purging 104

3.5 Characterisation 105
3.5.1 Density Measurement 105
3.5.2 Tensile test 106
3.5.3 Hardness test 107
3.5.4 Microstructure Observation 109
3.5.5 XRD Analysis 109

4 RESULTS AND DISCUSSION **111**

4.1 Raw materials analysis 111

4.2 Composite materials analysis 114

4.2.1 Phase I: Effect of weight percentage of magnesium in CPA 114

4.2.2 Phase II: Effect of variation of MnO_2 by changing its addition sequence in CPA 125

4.2.3 Phase III: Effect of variation in MnO_2 by changing its addition sequence along with the optimised magnesium from phase I study. 135

5 CONCLUSION **150**

6 FUTURE SCOPE OF THE WORK **153**

7 PAPER PUBLICATIONS **155**

Bibliography **159**

List of Figures

1.1 Generalised flow sheet of present work methodology 6

2.1 A classification of composite materials based on matrix materials 9

2.2 A classification of composite materials based on reinforcement materials 10

2.3 Different types of fiber reinforced composites 14

2.4 Laminar composite 15

2.5 Sandwich panel 16

2.6 Different composite manufacturing techniques 18

2.7 Single action compaction of powder mix 20

2.8 Sintering stages: (1) initiation of bonding at contact points; (2) formation of the necks; (3) reduction of pore size; and (4) development of the grain boundaries 21

2.9 Three particle model showing various diffusion mechanisms 21

2.10 Wettability phenomena 24

2.11 (a) Large θ gives non-wetting condition and (b) small θ gives wetting condition 24

2.12 Wetting phenomena between two different grains during liquid phase sintering occurs when θ_A and θ_B approach zero 25

2.13 Schematic diagram of spray deposition method 30

2.14 Line diagram of stir casting 31

2.15 Mechanical Stirring by impeller 31

2.16 Schematic illustration of infiltration process 32

2.17 Schematic illustrations of major infiltration processes: (a) spontaneous infiltration, (b) squeeze casting, (c) gas pressure infiltration, and (d) centrifugal infiltration 33

2.18 Schematic diagram of squeeze casting method 35

2.19 Classifications of the Squeeze Casting process 36

2.20 Direct and indirect squeeze casting: (a) Direct Squeeze Casting and (b) Indirect Squeeze Casting 36

2.21 Binary Al–Mg Phase Diagrams 38

2.22 Binary Al–Mn Phase Diagrams 39

2.23 Ternary phase diagram for Al-Mg-Mn liquidus projection 40

2.24 Ternary phase diagram for Al-Mg-Mn isothermal section at 750°C 41

2.25 Ternary phase diagram for Al-Mg-Mn isothermal section at 670°C 41

2.26 Ternary phase diagram for Al-Mg-Mn isothermal section at 400°C 42

2.27 Solidification structure of metal 43

2.28 Solidification Length Scale 43

2.29 Variation of the free energy with respect to the phase 44

2.30 Time-Temperature curve for the solidification of pure metal (cooling curve) 45

2.31 Computer simulated images of (a) 2D structure of casting and (b) 3D model of dendrite 46

2.32 (a) Variation of the free energy with respect to the particle radius during solidification and (b) Growth rate (G), nucleation rate (N) and temperature relation 47

2.33 Types of the solidification front (a) atomic scale and (b) microscale 48

2.34 (a) Types of the solidification front as a function of thermal gradient and rate of crystal growth and (b) Variation of the solidification front 49

2.35 Various solidification front and related microstructure. 49

2.36 (a) Formation of various interfacial front depending upon the thermal gradient and (b) The mechanism of dendritic growth arms 50

2.37 The principle aluminium alloys 55

2.38 Phase diagram of aluminium silicon alloy 60

2.39 Variation of properties with manganese amount 62

2.40 Variation of yield strength with different elements 63

2.41 Ex-situ composite and microstructures showing various phases in (a)AA7075Al−SiC and (b) AA7075Al − Al_2O_3 67

2.42 In-situ composite and microstructures showing various generated phases 68

2.43 Case I: Addition of MO in molten aluminium 69

2.44 Case II: Addition of MC in molten aluminium 69

2.45 Case III: Addition of MOC in molten aluminium 69

2.46 Applications of the Aluminium Metal Matrix Composites (AMMCs) in various fields 73

3.1 The schematic diagram of the experiment set-up used 86

3.2 Four blade turbine type stainless steel stirrer used in present work 87

3.3 Metallic die used in present work 87

3.4 (a) Raw CPA, (b) MnO_2 powder, (c) solid magnesium block and (d) fluxing powder and degassing tablet powder 88

3.5 Placing and setting up the crucible filled with charge materials in the resistance heating furnace . . 89

3.6 Resistance heating furnace before and after experimentation 89

3.7 Flow chart of experimental steps followed in phase I 90

3.8 Solidified AMMC in metallic die 92

3.9 Checking final yield after solidification of the AMMC (weight measurement) 92

3.10 Manual sample cutting by hacksaw 92

3.11 Preparation of hardness and microstructure samples 93

3.12 Preparation of tensile specimens 93

3.13 Flow chart of experimental steps followed in Sequence A of phase II 94

3.14 Flow chart of experimental steps followed in Sequence B of phase II 95

3.15 Flow chart of experimental steps followed in Sequence A of phase III 97

3.16 Flow chart of experimental steps followed in Sequence B of phase III 99

3.17 Measurement of density by Pycnometer 105

3.18 Monsanto-20 tensile testing machine and its accessories 106

3.19 Typical dimensions of the specimens for the tensile test 107

3.20 Brinell hardness testing machine 108

3.21 Scanning electron microscope 109

3.22 X-ray diffraction machine 110

4.1 Typical XRD pattern of (a) Commercially Pure Aluminium (CPA) and (b) MnO_2 powder in as received condition 112

4.2 (a) Optical microstructure of Commercially Pure Aluminium (CPA) and (b) SEM image of MnO_2 powder at 100X 113

4.3 Typical XRD pattern of Al-3 wt % Mg system 116

4.4 Variation of density in Al-Mg system 117

4.5 Variation of ductility in Al-Mg system 118

4.6 Variation of the hardness in Al-Mg system 119

4.7 Variation of the ultimate tensile strength in Al-Mg system 119

4.8 Optical Microstructure of (a) 0.05 wt % Mg, (b) 0.15 wt % Mg, (c) 0.5 wt % Mg, (d) 1wt % Mg, (e) 1.5 wt % Mg, and (f) 2 wt % Mg of Al-Mg system at 100x magnification (Without Etching) . . 121

4.9 Optical Microstructure of (a) 3 wt % Mg, (b) 4 wt % Mg, (c) 5 wt % Mg, (d) 6 wt % Mg and (e) 7 wt % Mg of Al-Mg system at 100x magnification (Without Etching) 122

4.10 SEM images of (a) 0.05 wt % Mg, (b) 0.15 wt % Mg, (c) 0.5 wt % Mg, (d) 1 wt % Mg, (e) 1.5 wt % Mg, and (f) 2 wt % Mg of Al-Mg system at 500x magnification (Without Etching) 123

4.11 SEM images of (a) 3 wt % Mg, (b) 4 wt % Mg, (c) 5 wt % Mg, (d) 6 wt % Mg and (e) 7 wt % Mg of Al-Mg system at 500x magnification (Without Etching) 124

4.12 Manganese recovery in Al-MnO_2 system 126

4.13 Fe/Si ratio of Al-MnO_2 system 126

4.14 Typical XRD pattern of Al-2.5 wt % MnO_2 system in sequence A of Al-MnO_2 system 127

4.15 Typical XRD pattern of Al-2.5 wt % MnO_2 system in sequence B of Al-MnO_2 system 128

4.16 Variations of density in sequence A and sequence B of Al-MnO_2 system 129

4.17 Variations of ductility in sequence A and sequence B of Al-MnO_2 system 130

4.18 Variations of hardness in sequence A and sequence B of Al-MnO_2 system 130

4.19 Variations of ultimate tensile strength in sequence A and sequence B of Al-MnO_2 system 131

4.20 Sequence A Optical microstructure of (a) 0.5 wt % MnO_2, (b) 1 wt % MnO_2, (c) 1.5 wt % MnO_2, (d) 2 wt % MnO_2, (e) 2.5 wt % MnO_2, (f) 3 wt % MnO_2, (g) 3.5 wt % MnO_2 and (h) 4 wt % MnO_2 of Al-MnO_2 system at 100x magnification (Without Etching) 132

4.21 Sequence B Optical microstructure of (a) 0.5 wt % MnO_2, (b) 1 wt % MnO_2, (c) 1.5 wt % MnO_2, (d) 2 wt % MnO_2, (e) 2.5 wt % MnO_2, (f) 3 wt % MnO_2, (g) 3.5 wt % MnO_2 and (h) 4 wt % MnO_2 of Al −MnO_2 system at 100x magnification (Without Etching) 133

4.22 SEM images of 2.5 wt % MnO_2 in sequence A at (a) 100x and (b) 500x magnification (Without Etching) 134

4.23 SEM images of 2.5 wt % MnO_2 in sequence B at (a) 100x and (b) 500x magnification (Without Etching) 134

4.24 Mn recovery in sequence A and sequence B of Al-3 wt % Mg-MnO_2 system. 136

4.25 Fe/Si ratio of Al-MnO_2 system 136

4.26 Typical X-ray diffraction patterns of 1 wt % MnO_2 in sequence A of Al-3 wt % Mg-MnO_2 system 137

4.27 Typical X-ray diffraction patterns of 2.5 wt % MnO_2 in sequence A of Al-3 wt % Mg-MnO_2 system 138

4.28 Typical X-ray diffraction patterns of 4 wt % MnO_2 in sequence A of Al-3 wt % Mg-MnO_2 system 139

4.29 Typical X-ray diffraction patterns of 1 wt % MnO_2 in sequence B of Al-3 wt % Mg-MnO_2 system 140

4.30 Typical X-ray diffraction patterns of 2.5 wt % MnO_2 in sequence B of Al-3 wt % Mg-MnO_2 system 141

4.31 Typical X-ray diffraction patterns of 4 wt % MnO_2 in sequence B of Al-3 wt % Mg-MnO_2 system 142

4.32 Variations of density in sequence A and B of Al-3 wt % Mg-MnO_2 system 143

4.33 Variations of ductility in sequence A and B Al-3 wt % Mg-MnO_2 system 143

4.34 Variations of hardness in sequence A and B of Al-3 wt % Mg-MnO_2 system 144

4.35 Variations of ultimate tensile strength in sequence A and B of Al-3 wt % Mg-MnO_2 system . . . 145

4.36 Optical microstructure of (a) 1 wt % MnO_2, (b) 2.5 wt % MnO_2 and (c) 4 wt % MnO_2 of Al-3 wt % Mg-MnO_2 system at 100x in sequence A (Without Etching) 146

4.37 SEM images of (a) 1 wt % MnO_2, (b) 2.5 wt % MnO_2 and (c) 4 wt % MnO_2 of Al-3 wt % Mg-MnO_2 system at 100x in sequence A (Without Etching) 147

4.38 Optical microstructure of (a) 1 wt % MnO_2, (b) 2.5 wt % MnO_2 and (c) 4 wt % MnO_2 of Al-3 wt % Mg-MnO_2 system at 100x in sequence B (Without Etching) 148

4.39 SEM images of (a) 1 wt % MnO_2, (b) 2.5 wt % MnO_2 and (c) 4 wt % MnO_2 of Al-3 wt % Mg-MnO_2 system at 100x in sequence B (Without Etching) 149

List of Tables

1.1 Parameters and properties of the research work 3

2.1 Availability of various elements from the earth crust 52

2.2 Generally adopted nomenclature for various degree of aluminium purity 52

2.3 Solid solubility of various elements in aluminium 53

2.4 The density of molten 99.996% aluminium 53

2.5 Designation of wrought aluminium alloys 55

2.6 Designation of cast aluminium alloys 58

2.7 Thermal expansion of aluminium 65

2.8 Mechanical properties of aluminium 65

2.9 Similar work reported by different researchers 81

3.1 Process Parameters 85

3.2 Specific gravity at 20°C of different compounds 103

4.1 Chemical composition of as supplied raw materials by Energy Dispersive Spectroscopy (EDS) 111

4.2 X-Ray diffraction values of as received commercially pure aluminium 113

4.3 X-Ray diffraction values of as received MnO_2 powder 113

4.4 Sieve analysis of MnO_2 powder 114

4.5 Chemical compositions of various Al-Mg systems by spectroscopy (Element Recovery) 115

4.6 X-Ray diffraction values of Al-3 wt % Mg sample 116

4.7 Chemical compositions of various Al-MnO_2 systems by spectroscopy (Element Recovery) 125

4.8 X-Ray diffraction values of Al-2.5 wt % MnO_2 system in sequence A 127

4.9 X-Ray diffraction values of Al-2.5 wt % MnO_2 system in sequence B 128

4.10 Chemical compositions of various Al-Mg-MnO_2 systems by spectroscopy 135

4.11 X-Ray diffraction values of Al-1 wt % MnO_2 system in sequence A 137

4.12 X-Ray diffraction values of Al-2.5 wt % MnO_2 system in sequence A 138

4.13 X-Ray diffraction values of Al-4 wt % MnO_2 system in sequence A 139

4.14 X-Ray diffraction values of Al-1 wt % MnO_2 system in sequence B 140

4.15 X-Ray diffraction values of Al-2.5 wt % MnO_2 system in sequence B 141

4.16 X-Ray diffraction values of Al-4 wt % MnO_2 system in sequence B 142

Background

Aluminium is most versatile metal because of unique combinations of properties which can be achieved through various routes and processing methods. This makes aluminium and its alloys most suitable for various applications from soft and thin wrapping foil to giant machinery parts such as aerospace, automobile, defence, domestic purpose, etc. since past many years. Many advance applications due to some of the excellent properties at low cost. Major properties which are concerned in aluminium and its alloys are strength, density, durability, machinability, etc. Aluminium can resist all types of oxidation compare to ferrous alloys. This is due to spontaneous formation of highly coherent and continuous inert Al_2O_3 thin film over the surface of the aluminium.

Composite is the tailor made materials so one can adjust the properties as per the requirements. Making a good interface between the matrix and reinforcements in the composite materials is prime requirement of the composite making industries. The stress which is applied on the composite should be shared across the interface. Making of interface becomes even more difficult when the reinforcement materials are immune to the chemical reactions. Ceramic particles are non reactive to even at higher temperature and hence there will be wettability issue.

Use of aluminium to make aluminium matrix composite is trend now-a-days either by powder metallurgy route or casting route. Aluminium as the matrix metal can serve many useful properties such as improvement in ductility, strength, toughness, hardness, etc. Aluminium Matrix Composites (AMCs) can be classified into four types depending on the type of reinforcement added into the matrix like:

- Particle-reinforced AMCs (P-AMCs)
- Whisker-or short fibre-reinforced AMCs (SF-AMCs)
- Continuous fibre-reinforced AMCs (CF-AMCs)
- Mono filament-reinforced AMCs (MF-AMCs)

There are various processing methods to fabricate the particle-reinforced aluminium metal matrix composites (P-AMCs). But based on the addition of reinforcement particles to the metal matrix, there are two different processing techniques like ex-situ and in-situ.

In ex-situ method, reinforcements are synthesised and modified externally before adding them into the liquid metal. The composites manufactured by ex-situ method always having poor

thermodynamic stability between matrix and reinforcement. They are also having poor high temperature properties. Several defects such as agglomeration and uneven microstructure can be seen in ex-situ composites [1].

In in-situ process, the metal matrix composite is developed by adding the reinforcement directly to the molten matrix material. The reinforcement is developed within the matrix by adding various ceramic particles such as oxides, carbides, nitrides or even halide salts to the molten matrix material. The reinforcement is developed by the exothermic reaction between the elements or their compounds with molten metal matrix. In in-situ method, reinforcements are synthesised and modified internally in the molten matrix metal where they transform to another thermodynamically stable phase. Such induced phases are more coherent to the matrix which improves the properties of the composite by principle of combined action. In-situ generated particles also have fine size, uniform distribution and improved interfacial bonding [1, 2].

In-situ technique is suitable to produce new composite materials that are not obtained by conventional methods. The in-situ process is having several advantages like uniform distribution of reinforcement, development of fine reinforcement particles and fine interface between the matrix and reinforcement. Synthesis of MMCs by casting is the economical processing route to develop in-situ metal matrix composites with the uniform distribution of the reinforcement.

Many researchers have put their efforts in past four decades to make in-situ aluminium matrix composites using various reinforcements such as particulate reinforcements like MnO_2 [2], Al_2O_3 [3-10], SiC [9, 11-13], SiO_2 [7, 14], ZrO_2 [8, 15], graphite [16-21], B_4C [22], Mica [23], TiB_2 [24], MoS_2 [25], TiO_2 [26], TiC [27, 28], Al_3Zr [28], Fe_3O_4 [30], Fe_2O_3 [31], ZnO [32], , carbon and boron fiber [33], rice hulk [34], etc. Higher mechanical properties can be achieved in all above cases as compared to the base alloy.

Problem Formulation

Metal matrix composite materials are known for their superior properties compared to the conventional metals and their alloys. Improved microstructures and mechanical properties of the composite materials are attributed to the type of matrix and reinforcement materials. Various chemical reactions between matrix and reinforcement at processing temperature generate new phases.

In present work, commercially pure aluminium (LM 0 grade) was used as the matrix material. Aluminium metal widely used for varieties of applications because of its -

- Low density (2.67 gm/cm^3),
- Ease of manufacturing due to low melting point and high ductility,
- High thermal and electrical conductivity,
- Excellent corrosion resistance,
- Low cost, etc.

MnO_2 powder was used as reinforcing constituent. MnO_2 is economical, easily available and strengthen the soft matrix likes aluminium. MnO_2 is generally immune to various chemical reactions and hence it requires the presence of wetting agents such as transition metals (Li, Mg, Ca, Ti, Zr and P). The purpose of these wetting agents is to improve the wetting characteristics of the immune (generally ceramic) reinforcement particles by reducing the surface tension [8].

Magnesium metal was used in current study as wetting agent for MnO_2 reinforcement. It does not only improve the wetting property but it also enhances the strength of the system by solid solution strengthening. Magnesium metal reacts with the aluminium matrix and reinforcement particles at the processing temperature and generates various in-situ phases. These in-situ phases are so small that they improve the mechanical properties such as strength and hardness. The strength can be increased due to dispersion strengthening effect. Magnesium metal is light in weight compare to the aluminium. Also, it is highly reactive with oxygen at high temperature.

Table 1: Parameters and properties studied

Sr. No.		Description
1	Parameters	Amount of reinforcement, Sequence of reinforcement addition,
2	Properties	Density, Ductility, Hardness, Tensile strength, Chemical analysis (spectroscopy) XRD and Microstructure.

There are many methods to generate in-situ composite materials. Most economical and less time consuming mass production method is the stir casting. Hence in present work, stir casting method was used to produce in-situ aluminium metal matrix composite (AMMC) materials. Four

blade stirrer was used in this work with fixed rotational speed. In stir casting method, due to continuous stirring effect, dispersion of generated in-situ phases is good which ultimately reduces the segregation problem. The microstructure and mechanical properties can be improved.

In this technique, attention is needed to avoid gas entrapment while addition of oxides and wetting agents. To decrease the chances of the porosity in the resultant in-situ composite, proper melt treatment has to be carried out before pouring of molten composite bath. Different parameters and properties studied are listed in following table 1.

Objectives of the work

Followings are the objectives of the research work:

1. To optimise the amount of wetting agent for commercially pure aluminium,
2. To study the variation of reinforcement and its sequence of addition,
3. To study generated in-situ phases after optimised the wetting agent and reinforcement oxides,
4. To study the microstructure and mechanical properties of generated in-situ composite material and
5. To compare the properties of existing material with new in-situ route.

Scope of the work

Making in-situ aluminium matrix composite (AMMC) materials requires extreme care. As mentioned above, many researchers have studied in-situ composite materials through various methods. During the review of the literatures, it was noted that most of all researchers have followed melting and casting route in which the reinforcement materials have been added after the melting of matrix system. In this sequence of addition, different defects were observed in resultant composite materials such as segregation and porosity. Some researchers have tried to use different sequence of addition (in Al-SiO_2 system by Rohatgi et. al. [7] and in Al-MnO_2 by Hamid et. al. [2]).

If reinforcement particles are heated at high temperature, it may pick the gases from an environment. It may generate poor interface between matrix and reinforcements while actual

processing. Thus addition of wetting agent is very important to change the surface chemistry of the reinforcement particles.

To understand the same problem and to increase the wettability of the particles TWO addition sequences of oxide were studied. The details of sequences are -

1. **Sequence A:** MnO_2 particles are added after the melting of the matrix metal (existing approach) and
2. **Sequence B:** MnO_2 particles are added before the melting of the matrix metal (new approach).

This comparative study between sequence A and sequence B revealed many interesting facts. Characterisation part of the research work shows the improvements in the properties by adopting new sequence compared to the existing sequence of the addition.

In industries, there is always requirement of the materials which are having improved properties. In this work, matrix metal was commercially pure aluminium (LM 0 grade) and reinforcement particles were MnO_2 powder which are not highly expensive. The manufacturing method adopted was the stir casting method which is again simple and economical method for mass production. This research work is not particular application oriented study but generated in-situ composite materials shows enhanced properties which can help to replace some existing materials.

Thesis Layout

This thesis is containing 07 chapters. The description of each chapter is given below:

1. **Chapter 1:** This chapter is describing about background of the work, problem evaluation and novelty, research gap, scope and objective of the work, importance research findings and research methodology used.

2. **Chapter 2:** This chapter contains the detailed literature review starting from the history of the composite materials, classification and manufacturing of composites, solidification behaviours, aluminium matrix composite materials, ex-situ and in-situ composites and applications of the composites in various fields. This chapter also contains the detailed review of relevant research articles which were published in various books and journals.

3. **Chapter 3:** In this chapter, detailed research methodology (procedure) is explained using simple flow charts. This chapter includes experimental set up details, various difficulties faced during melting and different characterisation methods.

4. **Chapter 4:** Results and related discussion was explained in this chapter. It starts form the raw materials analysis to final in-situ composite analysis (phase wise) with evidence in form of the tables, graphs and photographs.

5. **Chapter 5:** This is concluding chapter of the research work showing research output in brief.

6. **Chapter 6:** In this chapter, few points were discussed which remained untouch during this work. Also this chapter shows important information related to future scope of the work.

7. **Chapter 7:** This chapter shows the publications. Total 03 publications from each phase study were presented in this chapter. All these three publications are of international standard from which 02 are published in peer reviews SCOPUS journal whereas 01 paper was presented in international conference and published in its proceeding.

Experimental set up

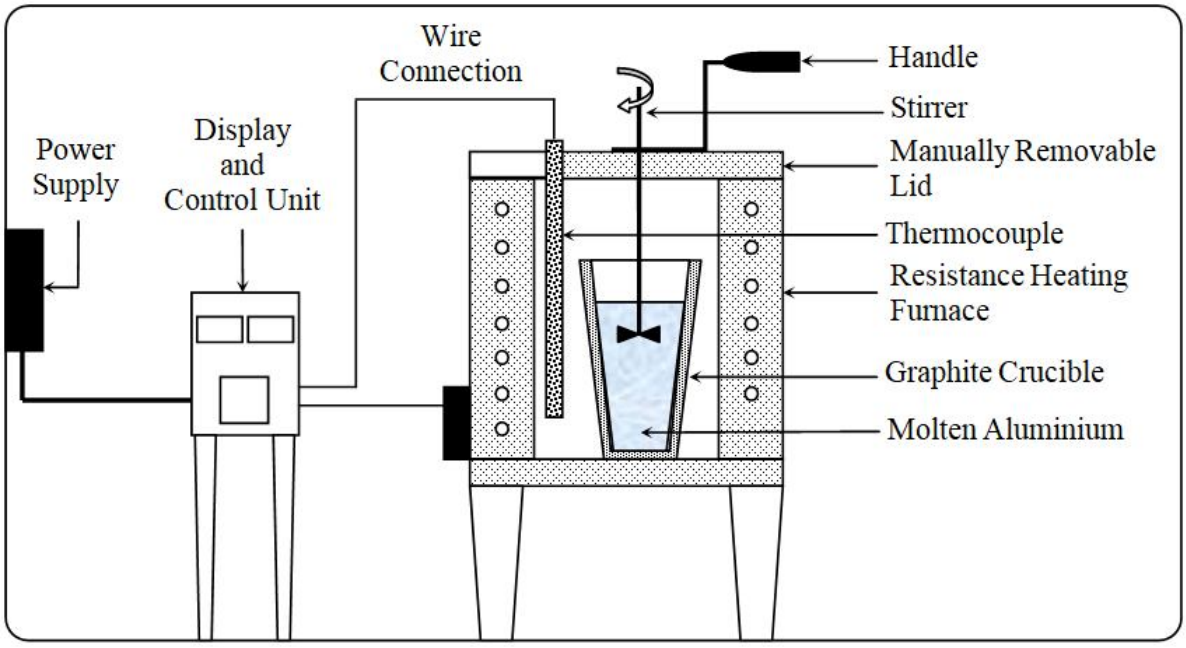

Figure 1: Schematic diagram of the experimental set up used in present study

The aluminium melting furnace used in this work is consists of the followings:

1. **Main melting zone:**

It is essentially square cross sectioned zone consisting outer mild steel wall and inner stainless steel wall having hole at the bottom side. In between outer and inner wall, heating coils are arranged as to provide resistance heating for the melting. Heating coils are made up of Kanthal wire.

2. **Thermocouple:**

It is Chromel-Alumel type thermocouple inserted into the melting zone to predict the temperature of the melt by displaying on to the temperature display panel in the degree Celsius unit.

3. **Temperature controller:**

It is connected to the heating coil as well as to the thermocouple. The automatic rely regulates the temperature to the preset limit and helps to maintain optimum temperature.

4. **Stirrer:**

It is typical turbine type four blade stainless steel stirrer which was used during stirring

5. **Speed and temperature controller:**

It is essentially used to control the speed of stirrer and the temperature of the bath via controlling the speed of motor. It is also used to indicate the actual speed of stirrer in working condition. This can be achieved by putting sensor near the bottom of the motor. Speed controller display shows the speed in the form of rpm and temperature of the bath.

6. **Metallic die:**

It is a metallic split die having 5 rod shape cavities in which liquid composite bath was poured and solidified

7. **Auxiliary Equipments:**

(a) *Al rod*
(b) *Toggle*
(c) *Strobometer or Techometer*
(d) *Muffle furnace or oven*
(e) *Drossing basket*
(f) *Spoon type rod*
(g) *Glows*
(h) *Oxy acetylene flame*
(i) *Hammer*
(j) *Hacksaw blade*

Research Methodology

In present work, melting and casting route was followed for fabrication of aluminium matrix composite with MnO_2 reinforcement. Following is the summarised flow chart of the experimental work presented in figure 2.

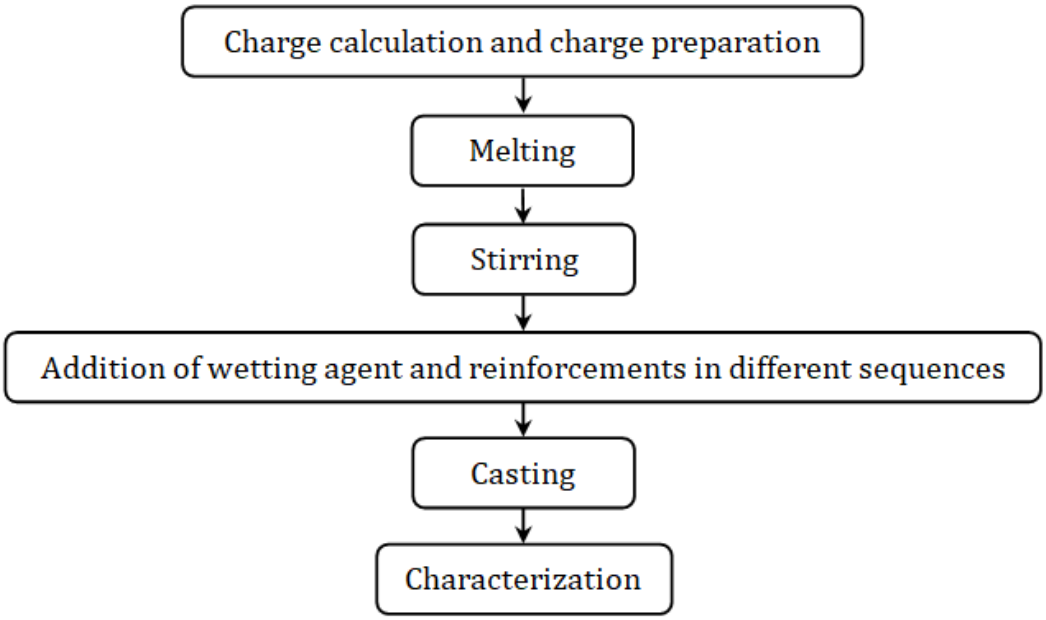

Figure 2: Generalised flow sheet of present work methodology.

Detailed methodology of each phase experimentation is explained in chapter 3 along with compassion between the existing addition sequence A with newly adopted addition sequence B.

Research Findings

The main aim of present research work is to improve the properties of commercially pure aluminium (CPA) by varying different parameters like amount of particulate reinforcement and its sequence of addition.

Selected reinforcement is MnO_2 because it is stable up to the temperature at around 500°C, above which decomposition take place [35] at 535°C and generates oxide particles. Optimization of magnesium was also checked for proper wetting of generated oxides or any other phases. The process parameters are reported in table 2. To check the effects of additions, detail analysis has been carried out in three different phases of experiments:

1. **Phase I:** Optimization of magnesium content into CPA

2. **Phase II:** Effect of variation of MnO_2 content by changing its addition sequence into CPA and

3. **Phase III:** Effect of variation of MnO_2 by changing its addition sequence along with optimised magnesium metal from phase I into CPA.

Table 2: Process Parameters

Sr. No.	Process Parameter	Process Variables		
		Phase I	*Phase II*	*Phase III*
1	Amount of Commercially Pure Al	1 kg	1 kg	1 kg
2	Processing temperature	720 °C	720 °C	720 °C
3	Time of processing	15 min	15 min	15 min
4	Stirrer speed	100 RPM	100 RPM	100 RPM
5	Amount of Commercially Pure Mg	0.05, 0.15, 0.5, 1, 1.5, 2, 3, 4, 5, 6 and 7*	--	3*
6	Amount of MnO_2	--	0.5, 1, 1.5, 2, 2.5, 3, 3.5 and 4*	1, 2.5 and 4*
7	Sequence of MnO_2 addition	--	A and B[#]	A and B[#]

*All compositions are in weight percent unless stated otherwise

[#]Sequence A: MnO_2 added after melting of commercially pure aluminium (conventional route) and Sequence B: MnO_2 added before melting of commercially pure aluminium (non-conventional route)

Phase I analysis – in Al−Mg system, magnesium metal was optimized with commercially pure aluminium (CPA) system. It was found that 3 wt % Mg was giving superior mechanical properties.

In phase II, analysis of Al-MnO_2 system, optimisation of MnO_2 powder was carried out with CPA. In this phase, both sequences A and B were followed to check its effect on final composite properties. It was noted that sequence B (MnO_2 powder added before the melting of matrix metal) and 2.5 wt % MnO_2 was giving best results compared to the sequence A (MnO_2 powder added after the melting of matrix metal).

Finally in phase III, with optimised magnesium metal plus the variations of MnO_2 by changing its addition sequences were analysed. It was found that the Al – 3 wt % Mg − 2.5 wt % MnO_2 system showed best results. In this study again sequence B was found the best compared to

sequence A. It was found that the in-situ phases which are generated in the matrix due to various chemical reactions are more favourable when we follow the sequence B.

After the processing of the aluminium matrix in-situ composites, various characterizations have been performed to investigate mechanical properties. Various mechanical properties such as ductility, density, hardness and strength were analysed as shown in table 1. Short summary of each phase such as variations in reinforcement additions, chemical analysis, mechanical property characterization, XRD analysis and microstructural evaluation are also discussed as following.

Phase I: Effect of weight percentage of magnesium in CPA

In phase I experiments, the amount of Mg was optimised through various trials. The amount of magnesium was varied from 0.05 to 7 wt % by keeping all other parameters constant. Phase I study involved the addition of commercially pure magnesium into commercially pure aluminium. As shown in table 2 of process parameters, **11 runs** of experiments were performed to check the effect of magnesium in CPA. One run of only CPA without magnesium addition with similar processing conditions was also taken for comparison purpose. These experiments were performed to determine the optimum level of magnesium for present CPA which used as matrix material. 700 gm of CPA, 720°C processing temperature and 15 minutes processing time were kept same for all the experiments. Magnesium amount was varied as 0.05, 0.15, 0.5, 1, 1.5, 2, 3, 4, 5, 6 and 7 wt %.

As the weight percentage of magnesium was increased, the recovery was also increased. At the same time, amount of oxygen was reduced. The amount of trace elements like Si, Mn and Fe were found minimum. Due to the presence of different elements, the presence of various phases was confirmed. Magnesium is strengthening element which forms solid solution strengthening into the CPA matrix. Hence it has improved various mechanical properties. X-ray diffraction (XRD) analysis of Al-3 wt % Mg system was carried out as it was showing maximum values of properties especially the strength. Presence of $MgSiO_3$, Al_2Mg_3, Mg-Si-O, Al_2O_3 and free Mg phases were confirmed. These in-situ phases were generated into the CPA matrix at processing temperature. Due to the presence of these multi in-situ phases, different mechanical properties were increased.

In present study of phase I, the density of the system was found decreasing throughout the variations of magnesium addition in CPA due to increasing the concentration of Mg which is having lower density (1.74 gm/ cm^3) compared to that of the aluminium (2.7 gm/ cm^3). Ductility

of overall system was also decreased as concentration of magnesium increased which was due to the formation of brittle phases such as oxides and carbides into the Al-Mg system as stated in microstructural analysis. Such phases are although light in weight but brittle in nature. Upon plastic deformation of the sample, such phases break into fine angular particles and act as stress raiser in the matrix. Hence as compared to the base metal, the ductility was not improved. Hardness (BHN) was found increasing starting from the initial experiments upto 3 wt % Mg. After 3 wt % Mg, hardness has continued to increase but the strength has dropped. The ultimate tensile strength (UTS) was found increasing initially and attained maximum value at 3 wt % of magnesium concentration. At 3 wt % Mg, highest UTS was achieved almost 217 MPa as compared to 115 MPa in base metal CPA. The UTS value was decreased to 167 MPa in 7 wt % of magnesium addition. Hence specific strength, i.e., strength to density ratio also increased from 42 kN-m/kg of base metal to 81 kN-m/kg at 3 wt % Mg and then decreased to 64 kN-m/kg at 7 wt % of magnesium concentration. After 4 wt % of magnesium, the slope of the graph became almost steady in case of tensile strength. Due to the formation of various intermetallics phases into the CPA matrix, strength was found increasing as compared to the base metal. As solubility of magnesium into aluminium decreases below 100°C, the solid solution strengthening effect can be observed maximum at 3 wt % of magnesium as compared to different experiments in this Al-Mg system.

Microstructural observation (both optical and scanning electron microscopy (SEM)) revealed that by increasing of magnesium amount, unreacted magnesium has observed at the grain boundaries along with other intermetallic phases. This leads to change in the morphology of the grain structure. Due to the formation of various solidification fronts, engulfment and pushing effects are responsible for the gathering of these micro particles at the grain boundaries. Such engulfment and pushing effect was found nominal up to 3 wt % of Mg and increased significantly after 3 wt % of Mg. Heavy cluster of intermetallic phases were observed in 4 wt %, 5 wt %, 6 wt % and 7 wt % of Mg. Unreacted magnesium also increased due to the limited solubility of magnesium metal in aluminium. Below 100°C, the solubility of magnesium reduces and becomes less than 3 wt %. But above 300°C, even 7 wt % Mg can be dissolved in aluminium melt easily as per the equilibrium phase diagram of Al-Mg. In this work, 3 wt % Mg can help to improve the wettability of the resulting in-situ intermetallic phases. Microstructures of the Al-Mg system show flawless grain structures. The presence of intermetallics was confirmed by XRD analysis. Microstructure of 3 wt % Mg is more uniform and equiaxed as compare to other microstructures. As the amount of magnesium increased, free magnesium was found in the structure as dark black phase.

Phase II: Effect of variation of MnO_2 by changing its addition sequence in CPA

In phase II, amount of reinforcing phase (MnO_2) was optimised without addition of magnesium as wetting agent. Phase II was conducted in two different approaches. In first approach named sequence A, MnO_2 reinforcing phase was added **after** melting of aluminium as conventionally practiced. In second approach which is named sequence B, the reinforcing phase MnO_2 was added **before** the melting of the aluminium, i.e. MnO_2 powder was mixed with the charging materials with solid CPA. During sequence B, due to gradual heating of MnO_2 particles and more time involvement in various reactions, it increased the recovery Mn from MnO_2. In this study, the addition of MnO_2 into commercially pure aluminium (CPA) was carried out without addition of commercially pure magnesium. As shown in table 2 of process parameters, there were **16 runs** of experiments carried out to check the effect of MnO_2 by changing the sequence of addition. In both the sequences, fixed amount of MnO_2 was varied like 0.5, 1, 1.5, 2, 2.5, 3, 3.5 and 4 wt %.

Recovery of manganese was found highest in 2.5 wt % MnO_2 of sequence B. It has been observed that Fe/Si ratio was found lowest in 2.5 wt % MnO_2 of sequence B. The X-Ray diffraction (XRD) analysis of 2.5 wt % MnO_2 was carried out for both sequences A and B experiments. Typical X-Ray pattern indicates the presence of oxides and complex carbides such as $FeSiO_3$, $MnAl_2O_3$, Mn_3AlC and Al_2O_3 into the CPA matrix. Raw MnO_2 contained the carbon and hence in resultant in-situ composite presence of complex carbides were seen. MnO_2 addition was very difficult beyond 2.5 wt %. The density of MnO_2 powder is very less as compared to CPA, we found floating of these powder on CPA liquid bath. The rejection of MnO_2 powder by the liquid bath was increased beyond 2.5 wt % level. This was the reason for choosing only 2.5 wt % MnO_2 sample for XRD analysis for sequence B.

The density results were dropping from the initial value throughout the addition of MnO_2 in sequence A and B. Generation of light weight phases such as MnO and $(Mn, Mg)_2SiO_4$ are responsible for decreasing the density of the system. The ductility values were remained almost same as no marginal changes were observed in the sequence A whereas it was found increasing in the sequence B. Hardness (BHN) distribution was remained almost unchanged in sequence A. But in sequence B, hardness value was increased as amount of MnO_2 added. The slight reduction in ultimate tensile strength (UTS) values were observed in sequence A while in sequence B, it was increased as the amount of MnO_2 was increased. Although the highest hardness values were observed in 2.5 wt % MnO_2 combination in the both sequences A and B whereas the highest

UTS was found in sequence A at 2.5 wt % MnO_2 compositions and at 2 wt % MnO_2 in sequence B.

Compare to sequence A, sequence B microstructures show more uniformity as far as morphologies of grains, grain boundaries and other resultant phases were concerned. By comparing both sequence results, the addition of MnO_2 as in sequence A showed more bulky grain boundaries and segregated phases whereas in sequence B, thin grain boundaries were observed. Also, the resultant phases were well distributed in sequence B.

Phase III: Effect of variation in MnO_2 by changing its addition sequence along with the optimised magnesium from phase I study

In phase III, combined effects of reinforcing phase MnO_2 along with wetting agent magnesium were studied. In this phase amount of magnesium was kept fixed at 3 wt. % which was optimised from phase I results while amount of MnO_2 was varied like 1, 2.5 and 4 wt. % for both sequences of addition. Addition of MnO_2 reinforcing phase was kept limited upto 4 wt. % because beyond this limit, it was observed that the liquid CPA rejected the excess powder of MnO_2. These experiments were carried out in two different approaches as indicted in phase II. In first approach (sequence A), MnO_2 added after melting of commercially pure aluminium whereas in second approach (sequence B), reinforcing phase was added before the melting of CPA. The results of both approaches were analysed in the next chapter. Formations of in-situ phases were confirmed which are improving various properties. Phase III study involved the addition of magnesium and MnO_2 both into commercially pure aluminium in two different sequences (A and B as mentioned in table 2). There were **total 06** runs of experiments, three in each sequence, have performed to check the effect of both magnesium and MnO_2 by changing its sequence of addition on various properties on CPA matrix. From phase I results, optimum value of magnesium in commercially pure aluminium was 3 wt %. Hence, keeping this result in mind, the magnesium content at 3 wt % was fixed, whereas MnO_2 concentration was varied as 0.5, 2.5 and 4 wt % in two different sequences (A and B).

Quantitative and qualitative analysis of various elements like Mg, Si, Mn and Fe recovered were performed. It is observed that Si and Fe are presence in raw materials. It was found that magnesium and manganese recoveries were higher in sequence B as compared to sequence A. Spectroscopy testing was performed for recovery of results. The presence of the in-situ complex carbide compounds such as Mg-Fe-SiO_3, $MnAl_2O_3$, Mg-Si-O, Al_2O_3, Mn_3AlC and Mg were

confirmed in the XRD patterns. It was noted that the peak height of Mn_3AlC in 2.5 wt % MnO_2 of sequence B experiments are higher as compared to all the combinations of sequence A experiments. It could be the main reason to have improved mechanical properties in this system following sequence B.

Presence of heavier and lighter phases in the matrix affects the level of density values of resultant composite material. In sequence B, lowest density was observed due to formation of light Al_2Mg_3 (molecular weight is 126.88 gm/mole) in-situ phase. In sequence A, formation of Al_3Mg_2 were observed which is comparatively heavier (molecular weight is 129.56 gm/ mole) as indicated in XRD analysis. Beyond 2.5 wt % MnO_2 addition, density values were increased in both the sequences A and B. Ductility values are found decreasing as the amount of MnO_2 addition increased. This was due to formation of hard phases in the matrix. Lowest reading of the ductility was noted in sequence A experiments. Overall both ductility and density were marginally lowered in both sequences A and B as compared to the base matrix material. In both A and B sequences, similar pattern of incremental hardness (BHN) were reported upto 2.5 wt % MnO_2 addition. Afterwards, hardness values were reduced. Maximum value of hardness property was reported in sequence B at 2.5 wt % MnO_2. It can be seen that in sequence A, the ultimate tensile strength (UTS) results were decreasing and found minimum at 2.5 wt % MnO_2 while in sequence B, the results were marginally higher and found maximum at 2.5 wt % MnO_2. Both hardness and tensile strength results in sequence B were found higher mainly due to in-situ formation of $MnAl_6$ along with cemented carbide Mn_3AlC. Formation of such phases is due to higher interaction time between MnO_2 and aluminium as it was added before melting of CPA. It means in sequence B, during entire melting procedure from room temperature to processing temperature, MnO_2 powder had more time to interact with CPA, from mushy stage to liquid stage. The presence of fine dispersoids in the soft aluminium matrix, acts as the barriers in the motion of dislocations. Thus it results into the dispersion strengthening which can be easily justified using classical Orowan theory. This phenomenon increases the flow stress of the entire composite system. The strengthening is generally found maximum where fine dispersoids are well distributed in the matrix.

Microstructure observations indicate the fineness of the intermetallics which were formed during processing. Precipitation and segregation of various Al-Mn intermetallics and carbide compounds were observed in the microstructures. Comparatively, in sequence B the intermetallics observed were well distributed throughout the matrix. In 1 wt % and 4 wt % MnO_2, more dense segregation was observed than 2.5 wt % MnO_2 systems. In the

microstructure, highest refinement was observed in Al-3 wt % Mg-2.5 wt % MnO_2 system in sequence B. More phase formation was appeared in Al-3 wt % Mg-1 wt % MnO_2. Also the distribution of Al-Mn complex carbide was found uniform.

Conclusion

The following final conclusions can be made from all above phases are:

1. From phase I study, Al-3 wt % Mg system was giving highest values of mechanical properties for present commercially pure Al metal.

2. From phase II study, the sequence B for MnO_2 addition is found more promising, i.e. when MnO_2 added in commercially pure aluminium before its melting by considering the changes in mechanical properties. The result of mechanical properties graph were steeper in sequence B compared to sequence A. In sequence B, the microstructures were much more refined and average value of Mn recovery is improved.

3. From phase III study, by keeping magnesium amount fixed at 3 wt % as optimized in phase I and after changing addition sequence the best sequence is B. In sequence B, the micromechanical results were more favourable then sequence A. Average recovered magnesium and manganese both were higher in sequence B as compared to A. It helps to promote the formation various in-situ phases as indicated in XRD analysis which ultimately strengthen the matrix.

Using above approach, the manufacturing of light weight - AMMCs can be promoted to achieve good micromechanical properties at lower cost as compared to the conventional materials and method of manufacturing.

References

[1] Dr. Kumar Sundaram. Ex-situ and in-situ metal matrix composites. https://sites.google.com/site/kumarspage/Home/research/ex-situ-and-in-situ-composites.

[2] Abdulhaqq A Hamid, SC Jain, PK Ghosh, and Subrata Ray. Processing, microstructure, and mechanical properties of cast in-situ Al (Mg, Mn)-Al_2O_3 (MnO_2) composite. *Metallurgical and Materials Transactions A*, 36(8):2211–2223, 2005.

[3] S.V. Kamat, J.P. Hirth, and R. Mehrabian. Mechanical properties of particulate-reinforced aluminum-matrix composites. *Acta Metallurgica*, 37(9):2395–2402, 1989.

[4] P.C. Maity, P.N. Chakraborty, and S.C. Panigrahi. Preparation of Al-$MgAl_2O_4$-MgO in situ particle-composites by addition of mno2 particles to molten Al-2 wt *Materials Letters*, 20(3):93–97, 1994.

[5] S.V Kamat, A.D Rollett, and J.P Hirth. Plastic deformation in Al-alloy matrix-alumina particulate composites. *Scripta Metallurgica et Materialia*, 25(1):27–32, 1991.

[6] MV Ravichandran, Krishna R Prasad, and ES Dwarakadasa. Fracture toughness evaluation of aluminium 4 % Mg-Al_2O_3 liquid-metallurgy particle composite. *Journal of materials science letters*, 11(8):452–456, 1992.

[7] PK Rohatgi, BC Pai, and S Ch Panda. Preparation of cast aluminium-silica particulate composites. *Journal of Materials Science*, 14(10):2277–2283, 1979.

[8] A Banerji, MK Surappa, and PK Rohatgi. Cast aluminum alloys containing dispersions of zircon particles. *Metallurgical Transactions B*, 14(2):273–283, 1983.

[9] MK Surappa and PK Rohatgi. Preparation and properties of cast aluminium-ceramic particle composites. *Journal of materials science*, 16(4):983–993, 1981.

[10] P.N. Kalu and T.R. McNelley. Microstructural refinement by thermomechanical treatment of a cast and extruded 6061 Al-Al_2O_3 composite. *Scripta Metallurgica et Materialia*, 25(4):853–858, 1991.

[11] AT Alpas and J Zhang. Effect of microstructure (particulate size and volume fraction) and counterface material on the sliding wear resistance of particulate-reinforced aluminum matrix composites. *Metallurgical and Materials Transactions A*, 25(5):969–983, 1994.

[12] Manish Roy, B Venkataraman, V Vetat Bhanuprasad, YR Mahajan, and G Sundararajan. The effect of participate reinforcement on the sliding wear behavior of aluminum matrix composites. *Metallurgical Transactions A*, 23(10):2833–2847, 1992.

[13] M Gupta, IA Ibrahim, FA Mohamed, and EJ Lavernia. Wetting and interfacial reactions in Al-*Li*-SiC_p metal matrix composites processed by spray atomization and deposition. *Journal of materials science*, 26(24):6673–6684, 1991.

[14] Akira Sato and Robert Mehrabian. Aluminum matrix composites: fabrication and properties. *Metallurgical Transactions B*, 7(3):443–451, 1976.

[15] A. Banerji, S.V. Prasad, M.K. Surappa, and P.K. Rohatgi. Abrasive wear of cast aluminium alloy-zircon particle composites. *Wear*, 82(2):141–151, 1982.

[16] SV Prasad and PK Rohatgi. Tribological properties of al alloy particle composites. *JOM*, 39(11):22–26, 1987.

[17] YB Liu, SC Lim, S Ray, and PK Rohatgi. Friction and wear of aluminium-graphite composites: the smearing process of graphite during sliding. *Wear*, 159(2):201–205, 1992.

[18] PK Rohatgi, S Ray, and Yun Liu. Tribological properties of metal matrix-graphite particle composites. *International materials reviews*, 37(1):129–152, 1992.

[19] P.K. Rohatgi and B.C. Pai. Seizure resistance of cast aluminium alloys containing dispersed graphite particles of various sizes. *Wear*, 59(2):323–332, 1980.

[20] S Mahdavi and F Akhlaghi. Effect of the graphite content on the tribological behavior of Al/Gr and Al/30SiC/Gr composites processed by in situ powder metallurgy (ipm) method. *Tribology Letters*, 44(1):1–12, 2011.

[21] BK Prasad. Microstructural modifications and improvement in properties of a hypoeutectic Al-Si alloy dispersed with graphite particles. *Journal of materials science letters*, 10(15):867–869, 1991.

[22] W. Kai, J.-M. Yang, and W.C. Harrigan. Mechanical behavior of B_4C particulate-reinforced 7091 aluminum composite. *Scripta Metallurgica*, 23(8):1277–1280, 1989.

[23] RT Bhat, PK Rohatgi, et al. Preparation of cast aluminium alloy-mica particle composites. *Journal of Materials Science*, 15(5):1241–1251, 1980.

[24] A.K. Kuruvilla, K.S. Prasad, V.V. Bhanuprasad, and Y.R. Mahajan. Microstructure-property correlation in $AlTiB_2$ (xd) composites. *Scripta Metallurgica et Materialia*, 24(5):873–878, 1990.

[25] Yunfeng Su, Yongsheng Zhang, Junjie Song, and Litian Hu. Novel approach to the fabrication of an alumina- MoS_2 self-lubricating composite via the in situ synthesis of nanosized MoS_2. ACS applied materials & interfaces, 9(36):30263–30266, 2017.

[26] P.C. Maity, S.C. Panigrahi, and P.N. Chakraborty. Preparation of aluminium-alumina in-situ particle composite by addition of titania to aluminium melt. *Scripta Metallurgica et Materialia*, 28(5):549–552, 1993.

[27] Purush Sahoo and Michael J. Koczak. Analysis of in situ formation of titanium carbide in aluminum alloys. *Materials Science and Engineering: A*, 144(1):37–44, 1991.

[28] XC Tong and AK Ghosh. Fabrication of in situ tic reinforced aluminum matrix composites. *Journal of materials science*, 36(16):4059–4069, 2001.

[29] Yu tao ZHAO, Song li ZHANG, and Gang CHEN. Aluminum matrix composites reinforced by in situ Al_2O_3 and Al_3Zr particles fabricated via magnetochemistry reaction. Transactions of *Nonferrous Metals Society of China*, 20(11):2129–2133, 2010.

[30] E Bayraktar and D Katundi. Development of a new aluminium matrix composite reinforced with iron oxide (fe. *Journal of achievements in materials and manufacturing engineering*, 38(1), 2010.

[31] R. Subramanian, C.G. McKamey, J.H. Schneibel, L.R. Buck, and P.A. Menchhofer. Iron aluminide–Al_2O_3 composites by in situ displacement reactions: processing and mechanical properties. *Materials Science and Engineering: A*, 254(1):119–128, 1998.

[32] Peng Yu, Cheng-Ji Deng, Nan-Gang Ma, and Dickon H.L. Ng. A new method of producing uniformly distributed alumina particles in al-based metal matrix composite. *Materials Letters*, 58(5):679–682, 2004.

[33] S. Senthil, M. Raguraman, and D. Thamarai Manalan. Manufacturing processes recent applications of aluminium metal matrix composite materials: A review. *Materials Today: Proceedings*, 45:5934–5938, 2021. International Conference on Mechanical, Electronics and Computer Engineering 2020: Materials Science.

[34] Md Rahat Hossain, Md Hasan Ali, Md Al Amin, Md Golam Kibria, and Md Shafiul Ferdous. Fabrication and performance test of aluminium alloy-rice husk ash hybrid metal matrix composite as industrial and construction material. *International Journal of Engineering Materials and Manufacture*, 2(4):94–102, 2017.

[35] Zaid B Jildeh, Jan Oberländer, Patrick Kirchner, Patrick H Wagner, and Michael J Schöning. Thermocatalytic behavior of manganese (iv) oxide as nanoporous material on the dissociation of a gas mixture containing hydrogen peroxide. *Nanomaterials*, 8(4):262, 2018.